GaInNAs Junctions for Next-Generation Concentrators: Progress and Prospects

D.J. Friedman, A.J. Ptak, S. R. Kurtz, J.F. Geisz, and J. Kiehl
National Renewable Energy Laboratory
1617 Cole Blvd, Golden, CO 80401, USA

ABSTRACT

We discuss progress in the development of GaInNAs junctions for application in next-generation multijunction concentrator cells. A significant development is the demonstration of near-100% internal quantum efficiencies in junctions grown by molecular-beam epitaxy. Testing at high currents validates the compatibility of these devices with concentrator operation. The efficiencies of several next-generation multijunction structures incorporating these state-of-the-art GaInNAs junctions are projected.

1. Introduction

GaInNAs has long been the leading candidate material for the 1-eV junction sought for future generations of ultrahigh-efficiency multijunction concentrator cells [1-4]. A 1-eV junction with GaAs-like minority-carrier properties lattice-matched to GaAs would make possible GaInP/GaAs/1-eV three junction structures with efficiencies >42% at 500 suns [5]. Unfortunately, the realization of this potential has been stymied by the low minority-carrier lifetime and mobility in GaInNAs, which adversely affects the quantum efficiency (QE) of GaInNAs junctions [2,4]. As a result, a conventional junction design relying on diffusion to collect the photocarriers, as is used for GaAs junctions, yields QEs in GaInNAs junctions which are typically on the order of 20% at best.

Greatly improved QEs can be achieved by use of field-aided collection in a wide depletion region, i.e. a p-i-n junction [2]. However, in growth of GaInNAs by the conventional metal-organic vapor-phase epitaxy (MOVPE) method, the low carrier concentrations of $\sim 10^{14}/cm^3$ required for wide depletion widths have not been achieved, presumably due at least in part to background doping by the carbon and hydrogen present in MOVPE. Hydrogen in GaInNAs is believed to stabilize Ga vacancies, which would be an additional source of background doping [6,7]. Background carrier concentrations for as-grown MOVPE material are typically $\sim 10^{17}/cm^3$, which can be lowered at best to $\sim 10^{15}/cm^3$ by annealing. For this reason, growth of GaInNAs by molecular-beam epitaxy (MBE) is a promising alternative to MOVPE, because of the low background carbon and hydrogen levels in MBE.

A complementary approach adapts the multijunction cell design for compatibility with the performance of existing GaInNAs junctions, directing the photocurrent to as many as six junctions to lower the current-matching requirements of the GaInNAs junction [8,9].

In the following sections, we discuss the implications of the development of the p-i-n GaInNAs junction. We first analyze the performance of such junctions at high currents, to confirm that these junctions are compatible with high-concentration operation. We then evaluate the projected efficiencies of the next-generation multijunction cell structures for the p-i-n GaInNAs junction, and compare these results to the efficiencies projected for the state-of-the-art MOVPE-grown GaInNAs junctions. In all cases, illumination under the low-AOD [10] spectrum is assumed.

2. p-i-n Junctions by MBE growth

Significant progress in GaInNAs junction performance was reported recently by Ptak, who grew GaInNAs junctions by elemental-source MBE [11,12]. These junctions have hole concentrations $p<10^{14}/cm^3$, resulting in p-i-n junctions with 3-µm-wide i-layers. Figure 1 shows the internal QE for one such junction [11], compared to the QE for one of the best junctions grown by the more conventionally-used method of MOVPE [13]. While the QE of the MOVPE junction is ~70%, the QE of the MBE junction is nearly ideal at ~95%. Also shown is a very simple model of the MBE junction's QE in which every photon absorbed in the 3-µm i-layer width W_i is assumed to be collected:

$$QE(h\nu) = 1 - \exp[-\alpha(h\nu) W_i] \quad (1)$$

where α is the absorption coefficient and $h\nu$ is the photon energy. Two different model curves are shown, one using a GaAs absorption coefficient [14], and the other using a GaInNAs absorption coefficient which was measured for 1.25-eV MOVPE-grown material [15]. In both cases, $\alpha(h\nu)$ was shifted rigidly in energy to match the 1.15-eV bandgap of the present junction. The band-edge region shows that the turn-on of $\alpha(h\nu)$ for the MBE-grown junction shown here is not quite as sharp as for GaAs, but is sharper than for

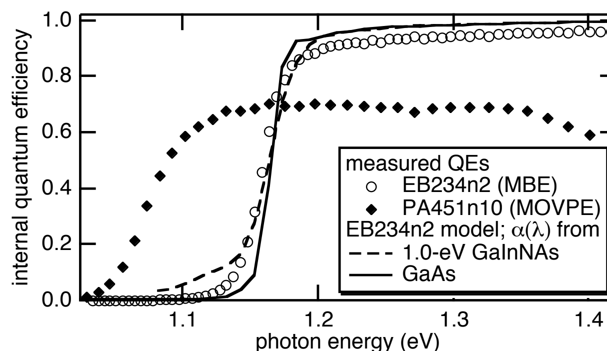

Figure 1. Internal QEs for state-of-the-art GaInNAs junctions grown by MBE [11] and MOVPE [15]. Also shown as dashed lines are simple models of the QE of the MBE junction.

MOVPE-grown GaInNAs. But clearly, the device's QE is nearly ideal. This is a significant proof-of-concept advance for GaInNAs junctions. The IV curve for this device is also of high quality by GaInNAs-junction standards, with a fill factor (FF) of 64% and an open-circuit voltage (V_{OC}) of 0.46 V at the illumination intensity of one sun filtered by GaAs. The corresponding short-circuit current (J_{SC}) for the low-AOD spectrum relevant to concentrators [10] is 9.5 mA/cm^2. This current, while not high enough to current-match to GaInP/GaAs, is more than sufficient to current-match the six-junction structure. Table 1 summarizes these parameters, as well as the corresponding parameters for the MOVPE-grown device of Fig. 1. In the next section we use these device parameters to project the efficiencies we would obtain with those junctions incorporated into next-generation multijunction structures.

Table 1. Description and operating parameters for the MOVPE- and MBE-grown GaInNAs junctions whose QEs are shown in Fig. 1.

Device ID	PA451n10	EB234n2
Grown by	MOVPE	MBE
Full description in Ref.	[13]	[11]
Absorber thickness (μm)	1	3
Absorber doping (cm^{-3})	2×10^{15}	$< 10^{14}$
Depletion width (μm)	0.5	3
E_g (eV)	1.062	1.152
V_{OC} (V)	0.38	0.46
Ideality factor *n*	1.35	1.65
QE(E_g+0.2 eV) (%)	69	96
J_{SC} filtered by GaAs (mA/cm^2)	9.0	9.5
Ge J_{SC} filtered by this device (mA/cm^2)	15.3	14.9

3. Multijunction Cell Efficiency Projections

Workers at Spectrolab [8] and Fraunhofer [9] have proposed and are developing a variety of five- and six-junction structures designed to have photocurrents low enough that present-day GaInNAs junctions do not limit the photocurrent in these structures. We limit our present discussion to the six-junction case, for simplicity. One example of such a design is GaInP/GaInP/GaAs/GaAs/GaInNAs/Ge ("6J#1"), illustrated schematically in Fig. 2. In this example, the photocurrent above the GaAs absorption is divided up among four junctions, rather than two as in the standard GaInP/GaAs/Ge ("3J#1") structure. The photocurrent is thus half of that in the standard 3J#1 structure, for which state-of-the-art J_{SC} is 13.9 mA/cm^2 [8]. Thus in this structure the GaInNAs junction need only exceed 7 mA/cm^2 for current matching. This current is readily achievable by state-of-the-art GaInNAs junctions, e.g. the junctions of Table 1. Furthermore, as indicated by the last entry in Table 1, both those junctions pass more than enough light to the underlying Ge junction.

While the 6J#1 structure demonstrates the idea of splitting the photocurrent, more sophisticated variants of 6J#1 which optimize the band gaps of the junctions to increase V_{OC} are likely to be of practical interest [8,9]. One such variant raises the band gaps of the first and third junctions by ~0.15–0.2 eV each [8], a structure which we will consider here and denote "6J#2". Other six-junction band gap combinations [9], as well as five-junction structures [8,9] have been suggested; for simplicity we focus our discussion on the 6J#1 and 6J#2 structures.

We now consider what the performance of these structures will be if GaInNAs junctions with the operating parameters in Table 1 can be incorporated into the multijunction structures. We can easily get a rough idea of the performance required of the GaInNAs junction in order for the 6J structures to exceed the efficiency of the 3J#1 benchmark device, assuming that every part of the structure other than the GaInNAs junction has the same nearly-ideal performance as has been achieved in 3J#1. Because the 6J#1 and #2 structures operate at half the current of 3J#1, they must generate more than twice the voltage of 3J#1 in order to beat 3J#1's efficiency. For 6J#1, this will be the case if the GaInNAs junction's V_{OC} is greater than 0.2 eV. This is the case for both the GaInNAs junctions of Fig. 1, whose V_{OC}s are 0.4 V or better. For 6J#2, because its V_{OC} is 0.35 eV greater than that of 6J#1, 6J#2's efficiency will beat that of the 3J#1 benchmark even if the GaInNAs junction's V_{OC} is zero.

An alternative to the six-junction structures is a three-junction structure, denoted 3J#3 in Fig. 2, in which the Ge junction of 3J#1 is replaced by a 1-eV GaInNAs junction [5]. For this 3J#3 structure, for current matching we require a GaInNAs junction with a 1-eV band gap and near-100% QE. The MBE junction of Fig. 1 satisfies the second criterion. We can ask what the performance of 3J#3 will be, assuming that we can lower the MBE GaInNAs bandgap to 1 eV without adversely affecting its QE (at present there is no reason to believe this will not be possible). The 3J#3 efficiency will exceed the 3J#1 benchmark efficiency if the GaInNAs junction in 3J#3 contributes more than the 0.2 V that the Ge junction contributes to 3J#1. Extrapolating from the parameters of the 1.15-eV MBE junction in Table 1, the V_{OC} for a 1.0-eV device would be 0.31 V. With that V_{OC}, 3J#3's efficiency should exceed 3J#1's benchmark.

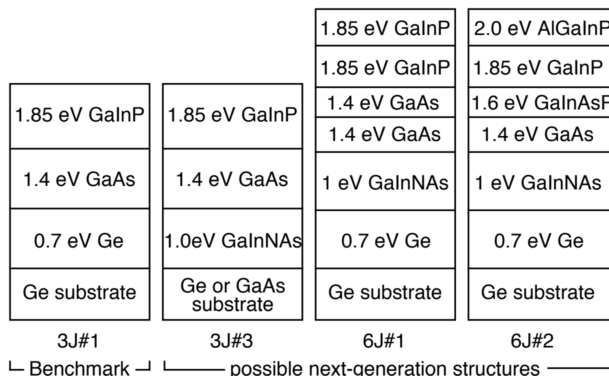

Figure 2. Schematic cross-sections of several possible next-generation multijunction structures and the present benchmark structure 3J#1.

To quantify the efficiencies we expect from these next-generation structures with our GaInNAs junctions, we use an empirical model [13] which calculates the IV curves for each junction as ideal diodes. The ideality factor, V_{OC}, and J_{SC} are the empirical inputs determining the ideal-diode curves. The resulting IV curve for the full multijunction structure is then calculated as the sum of the voltages of the individual junctions as a function of current, a procedure which correctly accounts for the fill factor. The efficiency of the multijunction structure is then taken from the maximum-power point of its IV curve. The 37.3%-efficient 3J#1 device reported by King [8] is taken as the starting point for the GaInP, GaAs, and Ge operating parameters. The AlGaInP and GaInAsP junctions in 6J#2 are taken to behave like GaInP and GaAs respectively, with the change in band gap giving an accompanying change in V_{OC}. The GaInNAs junction parameters are taken from the MOVPE and MBE devices of Fig. 1 – the efficiencies are calculated with both sets of parameters, for comparison purposes. For the 3J#3 structure, the band gap and accompanying V_{OC} of the 1.15-eV MBE GaInNAs junction was shifted down to 1.0 eV as discussed above. For 3J#3, the MOVPE junction was not considered because its QE is not high enough to current-match this structure. Grid coverage and series resistance are ignored.

The resulting efficiency projections are shown in Table 2. The 6J#1 structure is projected to have a 500-sun efficiency ~2 efficiency points higher than the 3J#1 benchmark at best. In practice, the gain in efficiency is likely to be less than this. The projected 500-sun efficiency of the 6J#2 structure is a more-compelling ~4 efficiency points higher than 3J#1. It remains to be seen how much of this projected gain can be realized given the difficulties of producing the required high-quality 2.0- and 1.6-eV junctions. Another challenge of this structure will come from the narrow range of photon energies feeding each junction, making it difficult to maintain current-matching as the operating temperature changes.

Table 2. Projected cell efficiencies for the cell structures discussed in the text, at 300K.

Device Structure†	GaInNAs junction properties taken from (see Table 1)	Efficiency (%)	
		1 sun	500 suns
3J#1		33.1	39.7
3J#3	EB234n2	33.6	41.0
6J#1	PA451n10 EB234n2	34.1 34.6	41.1 41.9
6J#2	PA451n10 EB234n2	36.5 37.0	43.5 44.3

†Device structures (see text for details):
3J#1: GaInP/GaAs/Ge
3J#3: GaInP/GaAs/GaInNAs
6J#1: GaInP/GaInP/GaAs/GaAs/GaInNAs/Ge
6J#3: AlGaInP/GaInP/GaInAsP/GaAs/GaInNAs/Ge

Finally, the simpler 3J#3 structure has a projected 500-sun efficiency 1.3 points higher than 3J#1. This gain is probably too small to pursue solely for the sake of cell efficiency alone. However, there are other potential advantages to this structure. It eliminates the necessity of the Ge junction, so that the photons of energy below 1 eV could be used for cogeneration rather than going to cell heating. The absence of the Ge junction also would allow 3J#3 to be grown on a semiinsulating substrate, enabling fabrication of monolithically integrated modules [16].

4. p-i-n Junctions at High Concentrations

While the wide, low-doped i-layer in the GaInNAs p-i-n structure gives a near-ideal QE, it also raises a concern that such structures might not be compatible with concentrator operation due to series resistance. To evaluate experimentally the effect of the i-layer on the concentrator operation of the GaInNAs junction, we chose a GaInNAs p-i-n junction EB252n12 similar to EB234n2 except for a slightly higher 1.28-eV band gap, and processed it with metal grids with a very high grid finger coverage to minimize the effects of "uninteresting" series resistance such as emitter and contact resistance. We then measured its light-IV characteristics on a pulsed solar simulator. Figure 3 shows the dark IV for this device, yielding a series resistance R_S=9 mΩ cm^2. Also shown is data for another device from the same wafer, completely metallized to even further reduce the series resistance losses from the emitter and grids. This fully metallized device has R_S=3 mΩ cm^2, and at least part of this is likely due to residual series resistance losses in the contacts. Thus, when we eliminate the contact and grid losses, which are irrelevant in the multijunction configuration that is the end goal for this device, we are left with an upper bound to the internal series resistance, $R_S \leq 3$ mΩ cm^2. This is very small: for a device operating at J=7 A/cm^2, corresponding to about 500 suns concentration, the ohmic drop due to this series resistance would be Jr_S=20 mV, a small fraction of the V_{OC}~0.6 V which this device would contribute.

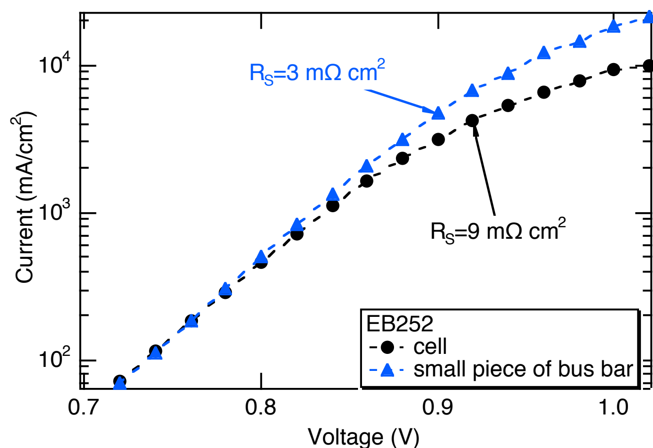

Figure 3. GaInNAs p-i-n junction dark-IV curves for the full cell including grids, and for a smaller piece which eliminates most of the series resistance losses in the emitter, fingers, and contact.

We also measured this device under illumination, using a pulsed solar simulator. Figure 4 shows the resulting data for the fill factor (FF) vs J_{SC}, i.e. vs concentration. The dashed line shows the fit to a simple series-resistance model with R_S=11 mΩ cm^2, in reasonable agreement with the 9 mΩ cm^2 deduced from the dark IV in Fig. 1. Figure 4 emphasizes that, even with contact and grid losses that will not be present in the multijunction configuration, the concentrator performance of this device is good. At 500 suns (indicated by the vertical dotted line in the figure), FF is only slightly less than at one sun, indicating that series resistance losses are not excessive.

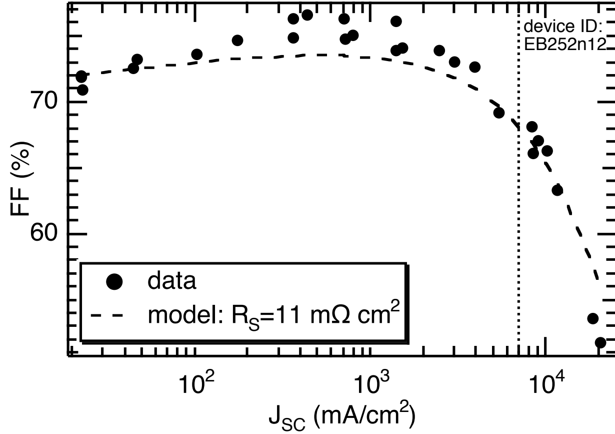

Figure 4. FF vs. J_{SC} for the GaInNAs junction of Fig. 1. The vertical dotted line is at the J_{SC} corresponding to 500 suns concentration.

Thus, the concern that the i-layer would contribute a large series resistance is not warranted. To understand this, we must consider the density of carriers injected into the i-layer at these high current densities. The volume of the i-layer is W_iA where A is the area. At a current I, carriers are being injected into this volume at rate I/e. These carriers have a lifetime τ. Thus the injected carrier density n_{INJ} is $n_{INJ}= \tau(I/e)/(W_iA) = J\tau/(eW_i)$. We have previously measured τ≈10ns by time-resolved photoluminescence for a GaInNAs layer with E_g=1.30 V, comparable to the E_g=1.28 eV for the device discussed here; therefore we take τ=10 ns. At a current density of, say, J=1 A/cm^2, with W_i=3μm, the resulting $n_{INJ}=2\times10^{14}$/cm^3. This is comparable to the doping density p_0 for this junction. Thus, for currents greater than about 1A/cm^2, we are well into the high-injection regime, where the density of carriers is $n\approx p\approx n_{INJ}$, rather than the low-injection case $n<<p\approx p_0$. The high-injection ohmic drop V_{Ohmic} across W_i is then

$$V_{Ohmic}=W_i^2/[\tau(\mu_p+\mu_n)]. \qquad (2)$$

It should be noted that a more rigorous treatment due to Hall gives a numerically similar result [17]. We take $\mu_p+\mu_n$=400 cm^2/Vs, typical for GaInNAs. Then, for our GaInNAs junction, V_{Ohmic}≈20 mV, a very small voltage drop which would not noticeably diminish the device performance.

5. Discussion

While the success of the MBE GaInNAs junction is an important proof of concept, one may ask how to proceed in incorporating this junction into a full multijunction structure, which is conventionally grown by MOVPE. It is hoped that study of the MBE junction will lead to a better understanding of the origin and behavior of the background carriers in the MOVPE material, making possible MOVPE-grown junctions with performance matching that of the MBE junction. If this path remains elusive, one can imagine growing the GaInNAs junction by MBE and then moving the wafer into an MOVPE reactor to grow the remaining junctions, but the economics of such a process may not be attractive. Also, in such a process the GaInNAs junction would be subject to extended heating and to indiffusion of hydrogen during the growth of the subsequent junctions, presenting the serious technical challenge of not degrading the high quality of the MBE junction during the growth of the subsequent junctions.

In a complementary approach, it may be possible to grow the entire multijunction structure by MBE. An MBE-grown version of the GaInP/GaAs two-junction cell with AM0 efficiencies of 21% has already been demonstrated on a production-scale reactor [18]. It seems reasonable to expect that further development would bring the efficiencies up to the state of the art. The economic practicality of this approach remains to be determined.

6. Conclusions

The performance of both MBE- and MOVPE-grown GaInNAs junctions has advanced to the point where they could be incorporated into specially designed multijunction designs such as the 6J#2 structure. Efficiency gains of four absolute efficiency points or more at 500 suns are projected for the 6J#2 structure compared to the standard benchmark 3J#1. Realizing these gains will be challenging, and the performance with variation in spectrum and temperature is a concern. The MBE junction could also be used in the simpler 3J#3 structure if the junction's band gap can be lowered to 1.0 eV while maintaining the near-ideal QE. The presence of the i-layer in these p-i-n junctions have been shown not to preclude concentrator operation.

Note added in proof: we thank Prof. Richard Schwartz for bringing to our attention Ref. 19, which discusses these concentrator fill factor issues at a high level of sophistication for Si concentrator cells.

7. References

[1] S.R. Kurtz, D. Myers, and J.M. Olson, "Projected Performance of Three- and Four-Junction Devices using GaAs and GaInP", *26th IEEE Photovoltaic Specialists Conference*, 1997, pp. 875-878.

[2] D.J. Friedman, J.F. Geisz, S.R. Kurtz, and J.M. Olson, "1-eV solar cells with GaInNAs active layer", *J. Cryst. Growth* **195**, 1998, pp. 409-415.

[3] D.J. Friedman, J.F. Geisz, S.R. Kurtz, and J.M. Olson, "1-eV GaInNAs Solar Cells for Ultrahigh-Efficiency

Multijunction Devices", *2nd World Conf. on Photovoltaic Energy Conversion*, 1998, pp. 3-7.

[4] S.R. Kurtz, A.A. Allerman, E.D. Jones, J.M. Gee, J.J. Banas, and B.E. Hammons, "InGaAsN solar cells with 1.0 eV band gap, lattice matched to GaAs", *Appl. Phys. Lett.* **74**, 1999, pp. 729-731.

[5] D.J. Friedman, S.R. Kurtz, and J.F. Geisz, "Analysis of the GainP/GaAs/1-eV/Ge cell and related structures for terrestrial concentrator application", *29th Photovoltaics Specialists Conference*, 2002, pp. 856-859.

[6] A. Janotti, S.-H. Wei, S.B. Zhang, S. Kurtz, and C.G.V.d. Walle, "Interactions between nitrogen, hydrogen, and gallium vacancies in $GaAs_{1-x}N_x$ alloys", *Phys. Rev. B.* **67**, 2003, pp. 1201.

[7] A.J. Ptak, S. Kurtz, K.G. Lynn, and M.H. Weber, "Positron annihilation spectroscopy study of vacancies in GaInNAs", *J. Vac. Sci. Technol. B* **22**, 2004, pp. 1584.

[8] R.R. King, C.M. Fetzer, K.M. Edmondson, D.C. Law, P.C. Colter, H.L. Cotal, R.A. Sherif, H. Yoon, T. Isshiki, D.D. Krut, G.S. Kinsey, J.H. Ermer, S. Kurtz, T. Moriarty, J. Kiehl, K. Emery, W.K. Metzger, R.K. Ahrenkiel, and N.H. Karam, "Metamorphic III-V materials, sublattice disorder, and multijunction solar cell approaches with over 37% efficiency", *19th European Photovoltaic Solar Energy Conference and Exhibition*, 2004, pp. 3587-3593.

[9] M. Meusel, F. Dimroth, C. Baur, G. Siefer, A.W. Bett, K. Volz-Koch, W. Stolz, G. Stroble, C. Signorini, and G. Hey, "European roadmap for the development of III-V multi-junction space solar cells", *19th European Photovoltaic Solar Energy Conference*, 2004, pp. 3581-3586.

[10] K. Emery, D. Myers, and S. Kurtz, "What is the Appropriate Reference Spectrum for Characterizing Concentrator Cells?" *29th IEEE Photovoltaic Specialists Conference*, 2002, pp. 840-843.

[11] A.J. Ptak, D.J. Friedman, C. Kramer, and M. Young, "Enhanced-depletion-width GaInNAs solar cells grown by molecular-beam epitaxy", *31st IEEE Photovoltaic Specialists Conference*, 2005,

[12] A.J. Ptak, D.J. Friedman, S. Kurtz, and R.C. Reedy, "Low-acceptor-concentration GaInNAs grown by molecular-beam epitaxy for high-current p-i-n solar cell applications", *J. Appl. Phys.* (2005, accepted for publication).

[13] D.J. Friedman and S.R. Kurtz, "Breakeven Criteria for the GaInNAs junction in GaInP/GaAs/GaInNAs/Ge four-junction solar cells", *Prog. Photovolt.* **10**, 2002, pp. 331-344.

[14] D.E. Aspnes, "Optical Functions of Intrinsic GaAs: Vacuum UV", *Properties of GaAs, 2nd Edition,* A. R. Peaker, Ed. (INSPEC, New York, 1990) pp. 156-160.

[15] S. Kurtz, J.F. Geisz, D.J. Friedman, J.M. Olson, A. Duda, N.H. Karam, R.R. King, J.H. Ermer, and D.E. Joslin, "Modeling of Electron Diffusion Length in GaInAsN Solar Cells", *28th IEEE Photovoltaic Specialists Conference*, 2000, pp. 1210-1213.

[16] J.S. Ward, A. Duda, T.J. Coutts, and S.R. Kurtz, "New concepts for high-intensity PV modules for use with dish concentrator systems", *15th NCPV Photovoltaics Program Review, AIP Conference Proceedings no. 462*, 1998, pp. 385-392.

[17] R.N. Hall, "Power Rectifiers and Transistors", *Proc. IRE* **40**, 1952, pp. 1512-1518.

[18] J. Lammasniemi, A.B. Kazantsev, R. Jaakkola, R. Aho, T. Mäkelä, M. Pessa, A. Ovtchinnikov, H. Asonen, A. Robben, and K. Bogus, "Characteristics of the first GaInP/GaAs cascade solar cells grown by a production-scale MBE system", *Second World Conference and Exhibition on Photovoltaic Energy Conversion*, 1998, pp. 1177.

[19] R. J. Schwartz, M. S. Lundstrom, and R. D. Nasby, "The degradation of high-intensity BSF solar-cell fill factors due to a loss of base conductivity modulation," *IEEE Trans. Electron. Devices* **ED-28**, 1981, pp. 264-269.